# The major autoantibody epitope on Factor H in atypical Hemolytic Uremic Syndrome is structurally different from its homologous site in Factor H related protein 1

**Arnab Bhattacharjee[1,2], Stefanie Reuter[3], Eszter Trojnár[4], Robert Kolodziejczyk[2,5], Harald Seeberger[3], Satu Hyvärinen[1], Barbara Uzonyi[6], Ágnes Szilágyi[4], Zoltán Prohászka[4], Adrian Goldman[2,5], Mihály Józsi[3,7], and T. Sakari Jokiranta[1]**

[1]*Department of Bacteriology and Immunology, Haartman Institute, and Research Programs Unit, Immunobiology, University of Helsinki, Finland*
[2]*Institute of Biotechnology, University of Helsinki, Finland*
[3]*Junior Research Group for Cellular Immunobiology, Leibniz Institute for Natural Product Research and Infection Biology - Hans Knöll Institute, Jena, Germany*
[4]*Research Laboratory, 3rd Department of Internal Medicine, Semmelweis University, Budapest, Hungary*
[5]*Department of Biosciences, Division of Biochemistry and Biotechnology, University of Helsinki, Helsinki, Finland*
[6]*MTA-ELTE Immunology Research Group, Department of Immunology, Eötvös Loránd University, Budapest, Hungary*
[7]*MTA-ELTE "Lendület" Complement Research Group, Department of Immunology, Eötvös Loránd University, Budapest, Hungary*

***Running title:** *Structural insight on CFHR1 deficiency in AI-aHUS*

Correspondence should be addressed to: Dr. Arnab Bhattacharjee, Haartman Institute; P.O. Box 21 (Haartmaninkatu 3); FIN-00014 University of Helsinki; Finland tel. +358 294 1911 fax. +358 294 191 26382. Email A.B: arnab.bhattacharjee@helsinki.fi or M.J: mihaly.jozsi@gmx.net

**Key words**: Thrombotic microangiopathy, complement regulation, autoimmunity, atypical hemolytic uremic syndrome, structure-function study

---

**Background:** The aHUS patients with autoantibodies against CFH lack CFHR1.
**Results:** The autoantibody epitope was mapped and the structure of the corresponding part of CFHR1 was solved.
**Conclusion:** The structural difference between the autoantigenic epitope of CFH and its homologous site in CFHR1 holds the key to the formation of autoantibodies in CFHR1 deficient aHUS patients.
**Significance:** A plausible explanation of the CFHR1 deficiency in autoimmune aHUS obtained

## ABSTRACT

**Atypical hemolytic uremic syndrome (aHUS) is characterized by complement attack against host cells due to mutations in complement proteins or autoantibodies against the complement regulator factor H (CFH). It is unknown why nearly all the patients with autoimmune aHUS lack CFH-related protein-1 (CFHR1). These patients have autoantibodies against CFH domains 19-20 ($CFH_{19-20}$) which are nearly identical to CFHR1 domains 4-5 ($CFHR1_{4-5}$). Here, binding site mapping of autoantibodies from seventeen patients using mutant $CFH_{19-20}$ constructs revealed an autoantibody epitope cluster within a loop on domain 20, next to the buried two residues different in $CFH_{19-20}$ and $CFHR1_{4-5}$. Crystal structure of $CFHR1_{4-5}$ revealed difference in conformation of the autoantigenic loop on the carboxyl-terminal domains of CFH and CFHR1 explaining variation in binding of autoantibodies from some aHUS patients to $CFH_{19-20}$ and $CFHR1_{4-5}$. The autoantigenic loop on CFH seems to be generally flexible as its conformation in previously published structures of $CFH_{19-20}$ bound to a microbial protein OspE and a sialic acid glycan is somewhat altered. Cumulatively our data suggest that association of CFHR1 deficiency with autoimmune aHUS could be owing to its structural difference to the autoantigenic CFH epitope suggesting a novel explanation for CFHR1 deficiency in pathogenesis of**

**autoimmune aHUS.**

## INTRODUCTION

aHUS is a rare and often fatal systemic disease, characterized by hemolytic anemia, thrombocytopenia, microvascular thrombosis, and kidney failure (1). It is associated with dysregulation of complement activation via either mutations, polymorphisms, or rearrangements in genes coding for various complement proteins (2). The mutations are mainly found in the gene coding for the complement regulator CFH (3,4), which mediates elimination of the central complement activation component C3b. We and others have shown how mutations in $CFH_{19-20}$ cause impaired regulation of C3b on host cells leading to complement attack against red blood cells, platelets, and endothelial cells as seen clinically in aHUS (5-8). Some aHUS cases, however, are caused by autoantibodies against CFH (CFH-AA). These antibodies have been identified in 5–11% of aHUS patients in different cohorts (9-13) but even 56% of 246 HUS patients have been reported with CFH-AA in India(14). Patients with the autoimmune form of aHUS nearly always lack certain CFH-related proteins, primarily CFHR1(10,15).

CFH and CFHRs are encoded by adjacent genes and form a protein family (supplemental Fig. S1)(16). CFHRs are composed of four to nine complement control protein (CCP) domains, also called short consensus repeats, and especially the two most carboxyl-terminal domains have relatively high sequence homologies with the carboxyl-terminal domains of CFH (supplemental Fig. S1)(16). There are only two residues different in the last two carboxyl terminal domains of CFH and CFHR1 (domains 19-20 and 4-5, respectively). The functional importance of these minor differences is obvious since the hybrid *CFH/CFHR1* genes producing fusion proteins $CFH_{1-18}/CFHR1_{4-5}$ or $CFHR1_{1-3}/CFH_{19-20}$ have been found in aHUS patients in the absence of other mutants or CFH-AA(4,17-19). The domains 19-20 of CFH are responsible for directing its complement regulatory activity to cell and extracellular matrix surfaces by binding simultaneously to both C3b and negatively charged glycosaminoglycans or sialic acid glycans on the surfaces (6,20,21). The autoantibodies of nearly all the patients with autoimmune aHUS recognize the carboxyl-terminus of CFH, and inhibit the physiological CFH-mediated protection of host cells from complement attack(10,11,13,22,23).

More than 90% of the patients with CFH-AA lack CFHR1 and CFHR3, resulting from a homozygous deletion of the genomic region containing both of them(10,12,13,15). Some patients have other rarer genetic alterations, including homozygous *CFHR1/CFHR4A* deletion (12), a combination of heterozygous *CFHR1/CFHR3* and *CFHR1/CFHR4A* deletions (12,13), or a combined heterozygous *CFHR1/CFHR3* deletion in the presence of a missense mutation in *CFHR1* (12). The common feature in all these genetic alterations is the deficiency of CFHR1 (24,25). However, CFH-AAs have also been described, although rarely, in patients having two normal copies of CFHR1 and CFHR3 but mutations in CFH, CFI, CD46, or C3 (12,13). CFH-AAs often cross-react with CFHR1 (13,23,26) but the exact location of the autoantibody site on CFHR1 has not been shown. On the basis of inhibition of autoantibody binding to CFHR1 by the mAb C18(26) and the sequence homology to the carboxyl-terminus of CFH it is, however, likely that the autoantibody binding site is within the last two domains of CFHR1, i.e. far away from its N-terminal dimerization site(27).

The reason for the association between CFH-AA and the CFHR1 deficiency has not been known till date. In this study we aimed at solving why deficiency of one molecule (CFHR1) predisposes to autoimmunity against another, highly homologous, molecule (CFH) in aHUS. We mapped the binding sites of CFH-AA within $CFH_{19-20}$ and compared the CFH-AA binding sites to the previously reported ligand binding sites on $CFH_{19-20}$. Since the autoantibody epitopes formed a cluster next to the residues that are different in the two carboxyl-terminal domains of CFH and CFHR1, we decided to solve and analyze the structure of $CFHR1_{4-5}$ and study the potential differences in antigenicity of those two molecules. We found structural differences in the autoantibody binding site of CFH domain 20 and the corresponding homologous site of CFHR1 domain 5. Based on these data a novel model is proposed hereby suggesting how immunization against CFH domain 20 could be linked to CFHR1 deficiency.

## EXPERIMENTAL PROCEDURES

**Proteins:** Cloning, expression and purification of the wild type (WT) and mutant $CFH_{19-20}$ proteins with the 14 single point mutations have been described earlier(5,7,28). Proper folding of the constructs has been verified for three mutants (Q1139A, R1203A and the double mutant D1119G/Q1139A) by solving the structures using X-ray crystallography(6,28,29) and for five mutants (R1182A, W1183L, K1188A, E1198A, and R1206A) by circular dichroism(30).

$CFHR1_{4-5}$ was generated by site directed mutagenesis of $CFH_{19-20}$ encoding DNA in pPICZαB vector (Invitrogen). The primer used to introduce the S1191L and V1197A mutations was CAG AAG CTT TAT TTG AGA ACA TCA GGT GAA GAA GCT TTT GTG. The mutations were confirmed by sequencing before expression of $CFHR1_{4-5}$ in *Pichia pastoris* (strain X-33) using 1% methanol induction as described previously(7).

Recombinant CFHR1, $CFH_{1-7}$, $CFH_{8-14}$, $CFH_{15-20}$ and CFHR4B were generated as described earlier(31,32).

CFH was bought from Merck Biosciences (Schwalbach, Germany). The mAb C18(33) was purchased from Enzo Life Sciences (Lörrach, Germany).

**Patients and blood samples:** The studies have been approved by the Research Ethics Committee of the Medical Faculty of Friedrich Schiller University and were performed in accordance with the Declaration of Helsinki.

Patients with aHUS were screened for CFH-AA using ELISA as described(9,11). All patients lacked the *CFHR1* and *CFHR3* genes and proteins except for patient 2, who had two copies of both genes, and patient 10 who carries a homozygous *CFHR1* deletion and is heterozygous for *CFHR3*. Three of the patients (patients 3, 7 and 8) have previously been described(22). Features of the used 17 patient sera containing CFH-AA are summarized in supplemental Fig. S2.

**Microtiter plate assays:** WT or mutant $CFH_{19-20}$ proteins (5 µg/ml) were coated to Nunc MaxiSorp plates (Thermo Scientific). Binding of patient sera (1:50-1:200 depending on the antibody titer) was analyzed as described[11]. Binding of mAb C18 (5 µg/ml) was detected using peroxidase-conjugated swine anti-mouse IgG.

Binding of the patient CFH-AA (sera diluted 1:100) to CFH, its recombinant fragments, CFHR1 and $CFHR1_{4-5}$ was compared as above using 250 nM immobilized recombinant proteins, plasma purified CFH (65 nM), or recombinant CFHR4B and albumin as negative controls (Fig. 2). Relative binding was calculated from representative datasets performed in triplicates.

The assay comparing binding avidity of $CFH_{19-20}$ and $CFHR1_{4-5}$ with the purified IgG of the patient 11 was done after coating $CFH_{19-20}$ (10 µg/ml) to Nunc MaxiSorp plates. After blocking (0.05% Tween-20 in PBS) for 120 min and washes (0.02% Tween-20 in PBS), 40 µl of patient IgG (3.8 µg/ml) and $CFH_{19-20}$, $CFHR1_{4-5}$, or $CFH_{5-7}$ was added in different dilutions and incubated for 120 min at 37°C followed by measuring IgG binding as described[11]. The experiment was performed three times in triplicates and the background subtracted data was normalized using the values obtained without an inhibitor (100% binding).

**Crystallization and solving the $CFHR1_{4-5}$ structure:** $CFHR1_{4-5}$ was crystallized at 293 K from hanging drops in the presence of 2 M ammonium sulphate and 0.1 M sodium acetate at pH 4.6. The cube shaped crystals appeared within 5 days and were cryo-protected by 25% glycerol (supplemented by the mother liquor). The diffraction data (to 2.9Å) were collected at the ESRF ID14-4 beamline (34) at 100K on a CCD ADSC Q315r detector at 0.979520 Å. The data were indexed and scaled using XDS (35). The structure of the $CFH_{19-20}$ mutant R1203A (PDB code 3KZJ,(28)) was used as a search model in Phaser(36), and two molecules of $CFHR1_{4-5}$ were identified in the asymmetric unit. After successive rounds of model building with Coot(37) and refinement in real space using 'phenix.refine' software(38) we could refine the structure to a higher precision than the initial model ($R_{work}/R_{free}$ = 0.20/0.26; supplemental Fig. S3). The last refinement cycles were done using TLS parameters (10 TLS groups). In the Ramachandran plot, 95% of the amino acid structures were within the most favoured region.

The superpositions of different structures and structural illustrations were prepared using

Pymol software (Schrödinger, Portland, USA). The surface charge distribution of both the molecules $CFHR1_{4-5}$ and $CFH_{19-20}$ was calculated using APBS(39) and the potentials on the solvent accessible surfaces were displayed in Pymol.

Coordinates and structure factors are available from the RCSB Protein Data Bank (http://www.pdb.org). The accession number is 4MUC for the crystal structure of the $CFHR1_{4-5}$.

**Statistical analyses.** Values are expressed as means ± SEM using GraphPad Prism software (version 6, La Jolla, CA). All curves and bar diagrams were made using the same software.

## RESULTS

**Mapping of the autoantibody binding residues on $CFH_{19-20}$.** Binding of IgG from sera of 17 aHUS patients with CFH-AA to 14 different $CFH_{19-20}$ mutants was tested (Fig. 1A). The binding data indicated a congruent tendency as follows. The binding of IgG from all the patients to the L1189R mutant was diminished at least 30% when compared to the wildtype (WT) $CFH_{19-20}$. IgG from fourteen patients showed at least 30% impaired binding to the E1198A mutant, and IgG from ten or eleven patients showed impaired binding to the $CFH_{19-20}$ mutants T1184R, K1186A, and K1188A when compared to WT $CFH_{19-20}$ (Fig. 1B). Binding of IgG from one to three patients was impaired to the D1119G, Q1139A, R1182A, W1183L, or R1210A mutants while binding of IgG from all the patients was similar to WT $CFH_{19-20}$ and the mutants W1157L, R1203A, R1206A, and R1215Q (Fig. 1B).

We also found that binding of the monoclonal antibody C18, which has previously been shown to have an epitope overlapping with that of several CFH-AAs(11,22), was diminished to the K1186A mutant (Fig. 1A). This antibody could efficiently inhibit binding of autoantibodies to $CFH_{19-20}$ from also those four individuals (patients 10, 11, 12, and 14) whose autoantibodies showed only moderately impaired binding to the five CFH mutants to which binding of autoantibodies from most of the patients was clearly impaired (data not shown). This indicates that the main binding site of the autoantibodies from also those patients is likely to be overlapping.

**The autoantibody-binding site overlaps with the heparin and common microbial binding sites.** Our previously solved crystal structure of $CFH_{19-20}$(7) was used to visualize location of the five residues of $CFH_{19-20}$ (T1184, K1186, K1188, L1189, and E1198) each of which were found to be involved in binding of CFH-AA from at least 10 out of 17 patients. These residues form a tightly packed cluster (diameter of approx. 11 Å) on one side of CFH domain 20 termed the "CFH-AA site" on domain 20 (Fig. 1C). When compared to the previously described functional sites on $CFH_{19-20}$ the CFH-AA site was clearly distinct from the two sites for C3b or C3d on domains 19 and 20(6,20) but adjacent to and partially overlapping with the site involved in binding of CFH to heparin and endothelial cells(5,40) (Fig. 1D) as well as the recently described common microbial binding site on CFH domain 20(29,30) (Fig. 1E).

**Binding of anti-CFH autoantibodies to the CFHR1 carboxyl-terminus.** On the basis of the previously solved structure of $CFH_{19-20}$, the two residues that are different in $CFH_{19-20}$ and $CFHR1_{4-5}$ (S1191 and V1197 of CFH) are buried beneath the identified CFH-AA site. Therefore we studied whether the difference of the two amino acids in the carboxyl-terminal domains of CFH and CFHR1 had an influence on binding of autoantibodies from the patient sera. The level of binding of antibodies from various patient sera to both $CFH_{19-20}$ and $CFHR1_{4-5}$ varied from patient to patient and this seemed to correlate to the antibody titer in the sera (Fig. S2). IgG from eight out of the ten CFH-AA patient samples that we had available enough for the analysis bound similarly to $CFHR1_{4-5}$, CFH, and $CFH_{19-20}$, while binding of autoantibodies from two of the samples (patients 2 and 9) was diminished to $CFHR1_{4-5}$ (Fig. 2 A-C). Next purified IgG fraction of the patient 11 was used to compare affinities of the autoantibodies to $CFH_{19-20}$ and $CFHR1_{4-5}$ using an inhibition assay. Binding of IgG was somewhat stronger to CFH in this assay (Fig. 2D, E) although a clear difference in binding to $CFH_{19-20}$ and $CFHR1_{4-5}$ could not be detected in the ELISA assay (Fig. 2B, C). Taken together, the results on difference in binding of CFH-AA to $CFH_{19-20}$ and $CFHR1_{4-5}$ indicated that the conformation of the CFH-AA site needs to be slightly different in CFH domain 20 and CFHR domain 5.

**Structures of the carboxyl-termini of CFHR1 and CFH are nearly identical.**

To detect possible differences in the CFH-AA site on $CFH_{19-20}$ and the corresponding site on CHFR1 we used X-ray crystallography to solve the structure of $CFHR1_{4-5}$. The structure was obtained as a homodimer at 2.9 Å resolution from a different space group (P622) than the previously published $CFH_{19-20}$ structures ($I4_122$)(7,28) (supplemental Fig. S3) but the structures aligned very well to each other (Fig. 3A). Superimposing the $CFHR1_{4-5}$ structure with the previously published structures of $CFH_{19-20}$ solved either as homotetramers (7), in complex with C3d (6), or in complex with the borrelial OspE protein (29) gave root mean square deviation (RMSD) of 0.5-1.1 Å for the 113 aligned Cα atoms, indicating that the structures were nearly identical. Also the charge potentials on the solvent accessible surface displayed at ±2 kT/e level on $CFHR1_{4-5}$ and $CFH_{19-20}$ were similar all around the molecules (Fig. 3B).

**Differences noticed in the structure of the CFH-AA site of $CFH_{19-20}$ and $CFHR1_{4-5}$.** The structures of $CFH_{19-20}$ and $CFHR1_{4-5}$ were seemingly identical but the detailed tertiary structure of the buried region containing the mutations S1191L and V1197A was naturally somewhat different (Fig. 3C). In addition, as expected on the basis of the differences observed in binding of certain autoantibodies and the previously reported functional differences of CFH/CFHR1 hybrid proteins, also the conformation of the CFH-AA site on $CFHR1_{4-5}$ was slightly different from that on $CFH_{19-20}$ (RMSD of backbone atoms of the loop region is 3Å); both the backbone and loops forming the CFH-AA site (R281-L288 of CFHR1 and R1182-L1189 of CFH, respectively) had a different orientation (Fig. 3D). The main difference in the backbone is formation of a short α-helix in the loop of $CFHR1_{4-5}$ while no prominent helix has been seen in this region in any of the solved structures of $CFH_{19-20}$. The orientation of some of the side chains was also clearly different as all the residues from R281 through L288 of $CFHR1_{4-5}$ were distinctively apart from the location of side chains of the corresponding residues of $CFH_{19-20}$ (from R1182 through L1189) (Fig. 3D). Interestingly only one of the two $CFHR1_{4-5}$ molecules in the same crystalline space showed the conformation that was dissimilar to the CFH-AA site on CFH domain 20 while the other $CFHR1_{4-5}$ molecule had the site similar to CFH. Since this indicated that the loop R281 through L288 of CFHR1 is flexible (or has two conformations), we next analyzed whether flexibility could be observed in the CFH-AA site of the previously published structures of $CFH_{19-20}$. Conformation of the loop R1182 through L1189 was somewhat different in free $CFH_{19-20}$ compared to the mutually similar conformation of $CFH_{19-20}$ in complex with either the microbial protein OspE (RMSD of the backbone of the loop residues: 2.7 Å), or the natural ligands C3d (RMSD of the backbone of the loop residues: 3.0 Å) or sialic acid glycan (RMSD of the backbone of the loop residues: 2.9 Å) (Fig. 3E, F). This conformation was also different from that of CFHR1 (RMSD of the backbone of the loop residues 3.0 Å). This indicates structural flexibility of the CFH-AA site upon binding of a ligand to the same domain (Fig. 3 E, F).

In order to exclude potential misinterpretation of the X-ray diffraction data of the CFH-AA site, we next compared the electron density maps (2mFo-DFc) of R1182-L1189 of $CFH_{19-20}$ (7) and R281-L288 of $CFHR1_{4-5}$ (Fig. 4). Clearly the model of $CFHR1_{4-5}$, but not of $CFH_{19-20}$, fits very well with the electron density map of $CFHR1_{4-5}$ in this region (Fig. 4A, B) while the corresponding region in the model of $CFH_{19-20}$, but not of $CFHR1_{4-5}$, fits well into the electron density map of $CFH_{19-20}$ (Fig. 4C, D). The real space correlation coefficients along with the B-factors of the above mentioned residues also showed normal behavior (supplemental Fig. S4) and there were no crystal contacts within this region in either the $CFHR1_{4-5}$ or $CFH_{19-20}$ structures.

**DISCUSSION**

Autoimmune-aHUS is an unusual autoimmune disease since it is associated with deficiency of a protein (CFHR1) homologous to the autoantigen (CFH). Therefore it offers an exceptional opportunity to study phenomena leading to antibody-associated autoimmunity. This study shows that the amino acid residues contributing to the binding sites of CFH-AA from seventeen patients with autoimmune aHUS form a cluster on domain 20 of CFH adjacent to the common microbial binding site. The differential binding of CFH-AA from two aHUS patient to $CFH_{19-20}$ and $CFHR1_{4-5}$, as also hinted previously(13,26), and the small but clear differences in the X-ray crystal structures of the

loop forming the autoantigenic epitope on CFH and CFHR1 indicate that the C-terminal domain of CFH and CFHR1 can have slightly different conformations. In addition, the conformation of the autoantigenic loop on CFH seems flexible since we noticed that the loop conformation is slightly different after binding of ligands to domain 20 or CFH in the previously published structures (21,29). The explanation why CFHR1 deficiency is associated with aHUS has been unexplained but the new results enabled an evaluation of the previously suggested and generation of a new hypothesis of induced autoantigenic neoepitope as an explanation for the association between CFHR1 deficiency and autoantibody formation against the common CFH-AA epitope on domain 20.

aHUS-associated mutations in the carboxyl-terminal domains of CFH have been to cause reduced binding of CFH to C3b or host cell surface structures such as glycosaminoglycans / heparin (5-7,41-43). aHUS-associated autoantibodies against $CFH_{19-20}$ cause uncontrolled complement attack against host cells and autoantibodies from some patients have been shown to impair CFH binding to C3b or to host cells (11). Location of the CFH-AA binding site we identified on domain 20 indicates that the autoantibodies are likely to block binding of CFH at least to glycosaminoglycans/heparin, owing to proximity of the CFH-AA site to the heparin-binding site. In addition, the location of the hemolysis-inducing aHUS mutation W1183L (26,44) next to the CFH-AA site (Fig. 3D) indicates the importance of the site in protecting host cells from complement. Although the C3b binding sites on CFH domains 19 and 20(6,20) are relatively distant from the CFH-AA binding site, the CFH-AAs might interfere with C3b binding owing to their large size as has been reported with the C18 mAb that we now and previously found to bind to the same region as the CFH-AAs (11)(Fig. 1A). Diminished binding of CFH to either the cell surface structures or C3b can lead to compromised protection of the plasma exposed host cells which has been reported widely in aHUS patients (1).

Upon close comparison of the conformation of the autoantigenic loop of CFH in the published crystal and NMR structures of $CFH_{19-20}$ (6,7,20,21,29,40,45) minor differences were noticed in the R1182-L1189 region of $CFH_{19-20}$ in complex with OspE (29), C3d (6), or a sialic acid glycan (21). RMSD of backbone atoms of the loop region was 2.7-3.0 Å when compared to $CFH_{19-20}$ alone (Fig. 3 E, F) Binding of $CFH_{19-20}$ to heparin tetrasaccharide has also been shown to cause chemical shift perturbations in NMR at the CFH-AA site (21,40). Taken together, it is likely that the conformation of the region is somewhat flexible. It seems possible that the corresponding site on CFHR1 is also structurally flexible since amongst the two monomers in the unit cell of the $CFHR1_{4-5}$ crystal conformation of the CFH-AA site of one monomer was similar to CFH and one was different (Figures 3 and 4). The key difference between CFH and CFHR1 could therefore be that CFHR1 takes the alternate conformation spontaneously while, on the basis of various crystal and NMR structures, $CFH_{19-20}$ takes a slightly altered conformation only upon binding of a ligand.

In the case of $CFHR1_{4-5}$, the difference with the $CFH_{19-20}$ structure being a crystal artifact is unlikely due to four reasons. First, only one of the monomers in a unit cell containing two $CFHR1_{4-5}$ molecules showed the structure which is considerably different from CFH domain 20 (see the PDB entry 4MUC) indicating structural flexibility in that loop of domain 5 of CFHR1. Second, there were no direct contacts found between the residues of the CFH-AA site (R281-L288) and the molecule in the neighboring crystal cell. Third, CFH-AA from two of the studied 10 patients bound differently to $CFH_{19-20}$ and $CFHR_{4-5}$ (Fig. 2C) indicating that there is a difference within the CFH-AA binding site of these molecules. Fourth, $CFHR1_{4-5}$ and $CFH_{19-20}$ have been reported to have functional difference (45), which is obvious since the fusion proteins $CFH_{1-18}$/FHR-$1_{4-5}$ and $CFHR1_{1-3}$/$CFH_{19-20}$ are associated with aHUS and have different functions from the normal full length CFH and CFHR1 (4,17-19). Since domain 19 of CFH and domain 4 of CFHR1 are identical it is deduced that the difference leading to the clinical disease is within the terminal domain of the fusion proteins leading to the inability to control complement on self surfaces (18). Our results suggest that the reason for the functional difference between the most carboxyl-terminal domains of CFH and CFHR1 is in their varied ability to bind to heparin or glycosaminoglycans on self cells since the loop which has different conformation in CFH and CFHR1 contains several of the heparin binding residues(5,40) (Fig. 1C, D and 3D).

Nearly all the patients with CFH-AA lack CFHR1 (12,13), and thus it is likely that the absence of CFHR1 imparts the risk of the CFH-AA generation. The risk for anti-CFH autoimmunity in the absence of CFHR1 is very high as the odds ratio is 442 (15). In this report we provide data for a structure-based molecular explanation to the phenomenon. The explanation is based on four observations in the current study. First, the binding sites of CFH-AA from the 17 analyzed individuals formed clearly a cluster, the CFH-AA site. Second, the CFH-AA site in CFH domain 20 is adjacent to the two buried residues (S1191 and V1197) that are different between $CFH_{19-20}$ and $CFHR1_{4-5}$. Third, although the crystal structures of $CFHR1_{4-5}$ and $CFH_{19-20}$ are similar owing to the 98.5% sequence identity between them there is a small structural difference exactly at the CFH-AA site on the loop R1182-L1189 of CFH (Fig. 3A, D). Fourth, a small conformational change has been detected within the autoantigenic loop upon binding of $CFH_{19-20}$ to a microbial protein (29), a sialic acid glycan (21), heparin, or C3d.

The two usual models to explain autoantibodies in general, an analogous epitope and a co-epitope model, are unable to explain the association of CFHR1 deficiency and CFH-AA binding to the CFH-AA site on domain 20. Thus, on the basis of the new data, we propose a novel explanation for the association of CFHR1 deficiency with the autoimmune disease. In this model, called the "induced neoepitope model", normal structure of the loop R1182-L1189 of CFH can be turned into an autoantigenic conformation upon induction by one or several ligands binding to that region of CFH domain 20 (Fig. 5). It has been reported that several kinds of infections can precede the autoimmune aHUS and this is concordant with our model since several microbial molecules are known to bind close to the autoantigenic epitope of CFH(29,30) and we observed from previously published data that $CFH_{19-20}$ in complex with OspE (29) has slightly altered conformation in this region.

Our model provides an explanation why immunization against the CFH-AA site could occur only in CFHR1-deficient individuals only since in normal individuals the presence of CFHR1 with an epitope similar to the hypothetical induced autoantigenic conformation of CFH would have guaranteed tolerance to that conformation of CFH. The model proposed here can explain also the other key biological phenomena described in autoimmune aHUS: association with infections (14,46), clustering of the autoantibody epitopes on domain 20 of CFH (Fig. 1), autoantibodies of IgG or IgA class (9,26) since foreign peptide for T-cell help could be provided by the microbial protein inducing the autoantigenic conformation, and polyclonality of the autoimmune response (23) since different epitopes on the autoantigenic loop could be recognized by various B-cell receptors.

In this report we show that CFH-AAs bind to a common site on the loop R1182-L1189 of CFH next to the buried two residues different in $CFH_{19-20}$ and $CFHR1_{4-5}$. The crystal structure of $CFHR1_{4-5}$ presented here also showed that the conformation of the autoantigenic loop is different on CFH and CFHR1. Taken together these data provided the basis for the suggested novel model (Fig. 5) to explain how CFHR1 deficiency is linked to CFH-AA formation.

**REFERENCES**


1. Noris, M., and Remuzzi, G. (2009) Atypical hemolytic-uremic syndrome. *N Engl J Med* **361**, 1676-1687
2. Sanchez-Corral, P., and Melgosa, M. (2010) Advances in understanding the aetiology of atypical Haemolytic Uraemic Syndrome. *Br J Haematol* **150**, 529-542
3. Zipfel, P. F., Edey, M., Heinen, S., Jozsi, M., Richter, H., Misselwitz, J., Hoppe, B., Routledge, D., Strain, L., Hughes, A. E., Goodship, J. A., Licht, C., Goodship, T. H., and Skerka, C. (2007) Deletion of complement factor H-related genes CFHR1 and CFHR3 is associated with atypical hemolytic uremic syndrome. *PLoS Genet* **3**, e41
4. Venables, J. P., Strain, L., Routledge, D., Bourn, D., Powell, H. M., Warwicker, P., Diaz-Torres, M. L., Sampson, A., Mead, P., Webb, M., Pirson, Y., Jackson, M. S., Hughes, A., Wood, K. M., Goodship, J. A., and Goodship, T. H. (2006) Atypical haemolytic uraemic syndrome associated with a hybrid complement gene. *PLoS Med* **3**, e431
5. Lehtinen, M. J., Rops, A. L., Isenman, D. E., van der Vlag, J., and Jokiranta, T. S. (2009) Mutations of factor H impair regulation of surface-bound C3b by three mechanisms in atypical hemolytic uremic syndrome. *J Biol Chem* **284**, 15650-15658
6. Kajander, T., Lehtinen, M. J., Hyvärinen, S., Bhattacharjee, A., Leung, E., Isenman, D. E., Meri, S., Goldman, A., and Jokiranta, T. S. (2011) Dual interaction of factor H with C3d and glycosaminoglycans in host-nonhost discrimination by complement. *Proc Natl Acad Sci U S A* **108**, 2897-2902
7. Jokiranta, T. S., Jaakola, V. P., Lehtinen, M. J., Pärepalo, M., Meri, S., and Goldman, A. (2006) Structure of complement factor H carboxyl-terminus reveals molecular basis of atypical haemolytic uremic syndrome. *EMBO J* **25**, 1784-1794
8. Ferreira, V. P., Herbert, A. P., Cortes, C., McKee, K. A., Blaum, B. S., Esswein, S. T., Uhrin, D., Barlow, P. N., Pangburn, M. K., and Kavanagh, D. (2009) The binding of factor H to a complex of physiological polyanions and C3b on cells is impaired in atypical hemolytic uremic syndrome. *J Immunol* **182**, 7009-7018
9. Dragon-Durey, M. A., Loirat, C., Cloarec, S., Macher, M. A., Blouin, J., Nivet, H., Weiss, L., Fridman, W. H., and Fremeaux-Bacchi, V. (2005) Anti-Factor H autoantibodies associated with atypical hemolytic uremic syndrome. *J Am Soc Nephrol* **16**, 555-563
10. Jozsi, M., Licht, C., Strobel, S., Zipfel, S. L., Richter, H., Heinen, S., Zipfel, P. F., and Skerka, C. (2008) Factor H autoantibodies in atypical hemolytic uremic syndrome correlate with CFHR1/CFHR3 deficiency. *Blood* **111**, 1512-1514
11. Jozsi, M., Strobel, S., Dahse, H. M., Liu, W. S., Hoyer, P. F., Oppermann, M., Skerka, C., and Zipfel, P. F. (2007) Anti factor H autoantibodies block C-terminal recognition function of factor H in hemolytic uremic syndrome. *Blood* **110**, 1516-1518
12. Abarrategui-Garrido, C., Martinez-Barricarte, R., Lopez-Trascasa, M., de Cordoba, S. R., and Sanchez-Corral, P. (2009) Characterization of complement factor H-related (CFHR) proteins in plasma reveals novel genetic variations of CFHR1 associated with atypical hemolytic uremic syndrome. *Blood* **114**, 4261-4271
13. Moore, I., Strain, L., Pappworth, I., Kavanagh, D., Barlow, P. N., Herbert, A. P., Schmidt, C. Q., Staniforth, S. J., Holmes, L. V., Ward, R., Morgan, L., Goodship, T. H., and Marchbank, K. J. (2010) Association of factor H autoantibodies with deletions of CFHR1, CFHR3, CFHR4, and with mutations in CFH, CFI, CD46, and C3 in patients with atypical hemolytic uremic syndrome. *Blood* **115**, 379-387
14. Sinha, A., Gulati, A., Saini, S., Blanc, C., Gupta, A., Gurjar, B. S., Saini, H., Kotresh, S. T., Ali, U., Bhatia, D., Ohri, A., Kumar, M., Agarwal, I., Gulati, S., Anand, K., Vijayakumar, M., Sinha, R., Sethi, S., Salmona, M., George, A., Bal, V., Singh, G., Dinda, A. K., Hari, P., Rath, S., Dragon-Durey, M. A., and Bagga, A. (2013) Prompt plasma exchanges and immunosuppressive treatment improves the outcomes of anti-factor H autoantibody-associated hemolytic uremic syndrome in children. *Kidney Int*
15. Dragon-Durey, M. A., Blanc, C., Marliot, F., Loirat, C., Blouin, J., Sautes-Fridman, C., Fridman, W. H., and Fremeaux-Bacchi, V. (2009) The high frequency of complement factor H related CFHR1 gene deletion is restricted to specific subgroups of patients with atypical

haemolytic uraemic syndrome. *J Med Genet* **46**, 447-450
16. Zipfel, P. F., Skerka, C., Hellwage, J., Jokiranta, S. T., Meri, S., Brade, V., Kraiczy, P., Noris, M., and Remuzzi, G. (2002) Factor H family proteins: on complement, microbes and human diseases. *Biochem Soc Trans* **30**, 971-978
17. Heinen, S., Sanchez-Corral, P., Jackson, M. S., Strain, L., Goodship, J. A., Kemp, E. J., Skerka, C., Jokiranta, T. S., Meyers, K., Wagner, E., Robitaille, P., Esparza-Gordillo, J., Rodriguez de Cordoba, S., Zipfel, P. F., and Goodship, T. H. (2006) De novo gene conversion in the RCA gene cluster (1q32) causes mutations in complement factor H associated with atypical hemolytic uremic syndrome. *Hum Mutat* **27**, 292-293
18. Eyler, S. J., Meyer, N. C., Zhang, Y., Xiao, X., Nester, C. M., and Smith, R. J. (2013) A novel hybrid CFHR1/CFH gene causes atypical hemolytic uremic syndrome. *Pediatr Nephrol*
19. Roumenina, L., Strain, L., Deury, D., Merle, N., Halbwachs-Mecarelli, L., Goodship, T., and Fremeaux-Bacchi, V. (2013) A prevalent CFHR1/FH reverse hybrid gene in aHUS patients induces deregulation of the alternative pathway. *Mol Immunol* **56**, 248
20. Morgan, H. P., Schmidt, C. Q., Guariento, M., Blaum, B. S., Gillespie, D., Herbert, A. P., Kavanagh, D., Mertens, H. D., Svergun, D. I., Johansson, C. M., Uhrin, D., Barlow, P. N., and Hannan, J. P. (2011) Structural basis for engagement by complement factor H of C3b on a self surface. *Nat Struct Mol Biol* **18**, 463-470
21. Blaum, B. S., Hannan, J. P., Herbert, A. P., Kavanagh, D., Uhrin, D., and Stehle, T. (2014) Structural basis for sialic acid-mediated self-recognition by complement factor H. *Nature Chemical Biology*, 2014 **advance online publication**
22. Strobel, S., Hoyer, P. F., Mache, C. J., Sulyok, E., Liu, W. S., Richter, H., Oppermann, M., Zipfel, P. F., and Jozsi, M. (2010) Functional analyses indicate a pathogenic role of factor H autoantibodies in atypical haemolytic uraemic syndrome. *Nephrology, dialysis, transplantation : official publication of the European Dialysis and Transplant Association - European Renal Association* **25**, 136-144
23. Blanc, C., Roumenina, L. T., Ashraf, Y., Hyvarinen, S., Sethi, S. K., Ranchin, B., Niaudet, P., Loirat, C., Gulati, A., Bagga, A., Fridman, W. H., Sautes-Fridman, C., Jokiranta, T. S., Fremeaux-Bacchi, V., and Dragon-Durey, M. A. (2012) Overall neutralization of complement factor H by autoantibodies in the acute phase of the autoimmune form of atypical hemolytic uremic syndrome. *J Immunol* **189**, 3528-3537
24. Hofer, J., Janecke, A. R., Zimmerhackl, L. B., Riedl, M., Rosales, A., Giner, T., Cortina, G., Haindl, C. J., Petzelberger, B., Pawlik, M., Jeller, V., Vester, U., Gadner, B., van Husen, M., Moritz, M. L., Wurzner, R., and Jungraithmayr, T. (2013) Complement Factor H-Related Protein 1 Deficiency and Factor H Antibodies in Pediatric Patients with Atypical Hemolytic Uremic Syndrome. *Clin J Am Soc Nephrol* **8**, 407-415
25. Holmes, L. V., Strain, L., Staniforth, S. J., Moore, I., Marchbank, K., Kavanagh, D., Goodship, J. A., Cordell, H. J., and Goodship, T. H. (2013) Determining the population frequency of the CFHR3/CFHR1 deletion at 1q32. *PLoS One* **8**, e60352
26. Strobel, S., Abarrategui-Garrido, C., Fariza-Requejo, E., Seeberger, H., Sanchez-Corral, P., and Jozsi, M. (2011) Factor H-related protein 1 neutralizes anti-factor H autoantibodies in autoimmune hemolytic uremic syndrome. *Kidney Int* **80**, 397-404
27. Goicoechea de Jorge, E., Caesar, J. J., Malik, T. H., Patel, M., Colledge, M., Johnson, S., Hakobyan, S., Morgan, B. P., Harris, C. L., Pickering, M. C., and Lea, S. M. (2013) Dimerization of complement factor H-related proteins modulates complement activation in vivo. *Proc Natl Acad Sci U S A* **110**, 4685-4690
28. Bhattacharjee, A., Lehtinen, M. J., Kajander, T., Goldman, A., and Jokiranta, T. S. (2010) Both domain 19 and domain 20 of factor H are involved in binding to complement C3b and C3d. *Mol Immunol* **47**, 1686-1691
29. Bhattacharjee, A., Oeemig, J. S., Kolodziejczyk, R., Meri, T., Kajander, T., Lehtinen, M. J., Iwai, H., Jokiranta, T. S., and Goldman, A. (2013) Structural Basis for Complement Evasion by Lyme Disease Pathogen Borrelia burgdorferi. *J Biol Chem* **288**, 18685-18695
30. Meri, T., Amdahl, H., Lehtinen, M. J., Hyvärinen, S., McDowell, J. V., Bhattacharjee, A., Meri, S., Marconi, R., Goldman, A., and Jokiranta, T. S. (2013) Microbes Bind Complement Inhibitor Factor H via a Common Site. *PLoS Pathog* **9**, e1003308

31. Hebecker, M., and Jozsi, M. (2012) Factor H-related protein 4 activates complement by serving as a platform for the assembly of alternative pathway C3 convertase via its interaction with C3b protein. *J Biol Chem* **287**, 19528-19536
32. Castiblanco-Valencia, M. M., Fraga, T. R., Silva, L. B., Monaris, D., Abreu, P. A., Strobel, S., Jozsi, M., Isaac, L., and Barbosa, A. S. (2012) Leptospiral immunoglobulin-like proteins interact with human complement regulators factor H, FHL-1, FHR-1, and C4BP. *J Infect Dis* **205**, 995-1004
33. Oppermann, M., Manuelian, T., Jozsi, M., Brandt, E., Jokiranta, T. S., Heinen, S., Meri, S., Skerka, C., Gotze, O., and Zipfel, P. F. (2006) The C-terminus of complement regulator Factor H mediates target recognition: evidence for a compact conformation of the native protein. *Clin Exp Immunol* **144**, 342-352
34. McCarthy, A. A., Brockhauser, S., Nurizzo, D., Theveneau, P., Mairs, T., Spruce, D., Guijarro, M., Lesourd, M., Ravelli, R. B., and McSweeney, S. (2009) A decade of user operation on the macromolecular crystallography MAD beamline ID14-4 at the ESRF. *J Synchrotron Radiat* **16**, 803-812
35. Kabsch, W. (2010) Xds. *Acta Crystallogr D Biol Crystallogr* **66**, 125-132
36. McCoy, A. J. (2007) Solving structures of protein complexes by molecular replacement with Phaser. *Acta Crystallogr D Biol Crystallogr* **63**, 32-41
37. Emsley, P., and Cowtan, K. (2004) Coot: model-building tools for molecular graphics. *Acta Crystallogr D Biol Crystallogr* **60**, 2126-2132
38. Adams, P. D., Grosse-Kunstleve, R. W., Hung, L. W., Ioerger, T. R., McCoy, A. J., Moriarty, N. W., Read, R. J., Sacchettini, J. C., Sauter, N. K., and Terwilliger, T. C. (2002) PHENIX: building new software for automated crystallographic structure determination. *Acta Crystallogr D Biol Crystallogr* **58**, 1948-1954
39. Baker, N. A., Sept, D., Joseph, S., Holst, M. J., and McCammon, J. A. (2001) Electrostatics of nanosystems: application to microtubules and the ribosome. *Proc Natl Acad Sci U S A* **98**, 10037-10041
40. Herbert, A. P., Uhrin, D., Lyon, M., Pangburn, M. K., and Barlow, P. N. (2006) Disease-associated sequence variations congregate in a polyanion recognition patch on human factor H revealed in three-dimensional structure. *J Biol Chem* **281**, 16512-16520
41. Manuelian, T., Hellwage, J., Meri, S., Caprioli, J., Noris, M., Heinen, S., Jozsi, M., Neumann, H. P., Remuzzi, G., and Zipfel, P. F. (2003) Mutations in factor H reduce binding affinity to C3b and heparin and surface attachment to endothelial cells in hemolytic uremic syndrome. *J Clin Invest* **111**, 1181-1190
42. Pangburn, M. K. (2002) Cutting edge: localization of the host recognition functions of complement factor H at the carboxyl-terminal: implications for hemolytic uremic syndrome. *J Immunol* **169**, 4702-4706
43. Jozsi, M., Heinen, S., Hartmann, A., Ostrowicz, C. W., Halbich, S., Richter, H., Kunert, A., Licht, C., Saunders, R. E., Perkins, S. J., Zipfel, P. F., and Skerka, C. (2006) Factor H and atypical hemolytic uremic syndrome: mutations in the C-terminus cause structural changes and defective recognition functions. *J Am Soc Nephrol* **17**, 170-177
44. Sanchez-Corral, P., Gonzalez-Rubio, C., Rodriguez de Cordoba, S., and Lopez-Trascasa, M. (2004) Functional analysis in serum from atypical Hemolytic Uremic Syndrome patients reveals impaired protection of host cells associated with mutations in factor H. *Mol Immunol* **41**, 81-84
45. Herbert, A. P., Kavanagh, D., Johansson, C., Morgan, H. P., Blaum, B. S., Hannan, J. P., Barlow, P. N., and Uhrin, D. (2012) Structural and functional characterization of the product of disease-related factor H gene conversion. *Biochemistry* **51**, 1874-1884
46. Dragon-Durey, M. A., Sethi, S. K., Bagga, A., Blanc, C., Blouin, J., Ranchin, B., Andre, J. L., Takagi, N., Cheong, H. I., Hari, P., Le Quintrec, M., Niaudet, P., Loirat, C., Fridman, W. H., and Fremeaux-Bacchi, V. (2010) Clinical features of anti-factor H autoantibody-associated hemolytic uremic syndrome. *J Am Soc Nephrol* **21**, 2180-2187

**ACKNOWLEDGEMENTS**

We acknowledge Kirsti Widing and Marjo Rissanen for excellent technical assistance. We also thank ESRF for beamtime on the ID14-4 beamline and Seija Mäki in the Biocenter Finland crystallization facility. AG and TSJ acknowledge research grants from the Sigrid Jusélius foundation and the Academy of Finland (grants 1252206 (AG), 128646, 255922, 259793 (TSJ)) ZP was supported by a grant from the Hungarian Scientific Research Fund (OTKA 100687). MJ gratefully acknowledges research grants from the German Research Fund (JO 844/1-1), the Hungarian Scientific Research Fund (OTKA 109055) and the Hungarian Academy of Sciences (LP2012-43). AB thanks Dr. Taru Meri for having very fruitful discussions that enriched the article. AB and TSJ also thank Prof. Seppo Meri for constructive comments on the autoimmunity model.

**Authorship:**

A.B., M.J. and T.S.J. designed the research; A.B., S.R., H.S, B.U., M.J. and E.T. performed the research; A.B., S.H., M.J., A.S, B.U, Z.P., R.K. and A.G contributed to new reagents/analytic tools; A.B., Z.P., A.G, M.J. and T.S.J. analyzed the data; A.B. and T.S.J. coordinated the project and wrote the paper with help from M.J. and Z.P.

**FOOTNOTES**

Coordinates and structure factors are available from the RCSB Protein Data Bank (http://www.pdb.org). The accession number is 4MUC for the crystal structure of the $CFHR1_{4-5}$.
Correspondence and requests for materials should be addressed to A.B. (arnab.bhattacharjee@helsinki.fi) or M.J. (mihaly.jozsi@gmx.net)

The abbreviations used are: aHUS, atypical hemolytic uremic syndrome; AI-aHUS, autoimmune atypical hemolytic uremic syndrome; CCP, complement control protein domain; CFH, complement factor H; CFHR1, complement factor H-related protein-1; CFH-AA, anti-CFH autoantibodies; WT, wild type.

**FIGURE LEGENDS**

**FIGURE 1**. Mapping of CFH-AA binding region on domains 19-20 of CFH. (A) Binding of IgG from seventeen aHUS patients and a monoclonal anti-CFH antibody C18 to 14 $CFH_{19-20}$ constructs with various single point mutations in relation to binding to the WT $CFH_{19-20}$. The error bars indicate standard error of the mean and the level of WT binding is indicated by a dotted line. (B) Comparison of the autoantibody binding epitopes by identification of the mutations that impaired binding of patient IgG at least by 30% (indicated by '↓'). (C) Location of the residues involved in binding of autoantibodies to $CFH_{19-20}$ as indicated in dark grey and annotated on a previously published structure of $CFH_{19-20}$ (PDB code 2G7I)(7); location of W1183 is indicated with stripes. (D) For comparison, location of the residues involved in binding of $CFH_{19-20}$ to heparin(5,40), and (E) location of the residues involved in the common microbial binding site on $CFH_{19-20}$ (30) are indicated in dark grey.

**FIGURE 2**. Binding of autoantibodies from autoimmune aHUS patients to CFH and CFHR1. (A) Binding of the autoantibodies to CFH (full length) and its fragments $CFH_{1-7}$, $CFH_{8-14}$, $CFH_{15-20}$, and $CFH_{19-20}$. (B) Binding of the IgG autoantibodies to CFH, CFHR1 (full length), $CFHR1_{4-5}$, and CFHR4B (full length). Human serum albumin (HSA) and/or normal human serum (NHS) were used as negative controls and polyclonal goat anti-CFH antibody as a positive control. (C) A bar diagram

elucidating the relative binding ratio of the patient autoantibodies to $CFH_{19-20}$ and $CFHR1_{4-5}$. The error bars indicate the standard error of the mean. CFHR1 deficiency of each patient is shown below the columns of panel C. (D) Binding of purified IgG from the patient 11 to $CFH_{19-20}$ was tested in the presence of increasing concentration of $CFH_{19-20}$ or $CFHR1_{4-5}$. $CFH_{5-7}$ was used as a negative control. (E) Bar diagram of the concentration of $CFH_{19-20}$ or $CFHR1_{4-5}$ needed for 50% inhibition (IC50) obtained from three independent experiments performed in triplicates. The error bars indicate the standard error of the mean.

**FIGURE 3**. Crystal structure of $CFHR1_{4-5}$ and its comparison with the previously solved structure of $CFH_{19-20}$. (A) Structural superposition of the two molecules of $CFHR1_{4-5}$ (orange and yellow) found in the asymmetric unit along with $CFH_{19-20}$ (grey) shown in a cartoon model. (B) Comparison of the surface charge potentials of $CFHR1_{4-5}$ and $CFH_{19-20}$. Potentials on the solvent accessible surfaces were calculated and displayed at ±2 kT/e level on both the structures after modeling all of the missing side chains of the previously published structure of $CFH_{19-20}$ (PDB code 2G7I)(7). (C) A close view of the two residues different in the amino acid sequences of these two protein constructs with the 2mFo-DFc electron density map of $CFHR1_{4-5}$ shown. (D) A close view of the region in which the tertiary structures of $CFHR1_{4-5}$ and $CFH_{19-20}$ were dissimilar (residues R1182 through L1189 of $CFH_{19-20}$ and the corresponding residues R281 through L288 of $CFHR1_{4-5}$) with backbone and side chain atoms shown using a stick model. This region corresponds to the CFH-AA binding site shown in Fig. 1. (E) A cartoon representation of the structural superposition of $CFHR1_{4-5}$ (orange: PDB code 4MUC) with $CFH_{19-20}$ (grey: PDB code 2G7I (7)), $CFH_{19-20}$ in complex with a sialic acid glycan and C3d (slate: PDB code 4ONT (21)), and CFH19-20 in complex with OspE (turquoise: PDB code 4J38 (29)). (F) A close view of the residues R1182 through L1189 of $CFH_{19-20}$ and the corresponding homologous residues of $CFHR1_{4-5}$ with a color scheme same as seen in Figure 3, E.

**FIGURE 4**. Comparison of the models and 2mFo-DFc electron density maps of the CFH-AA binding site of $CFH_{19-20}$ and the corresponding site of $CFHR1_{4-5}$. (A) The $CFHR1_{4-5}$ loop region (R281-L288), or (B) the $CFH_{19-20}$ loop region (R1182-L1189) are shown with the $CFHR1_{4-5}$ 2mFo-DFc electron density map. (C) The $CFH_{19-20}$ loop region (R1182-L1189), or (D) the $CFHR1_{4-5}$ loop region (R281-L288) are shown with the $CFH_{19-20}$ 2mFo-DFc electron density map. Stick model and electron density map of $CFHR1_{4-5}$ are displayed in orange and those of $CFH_{19-20}$ in grey.

**FIGURE 5**. A schematic illustration of a model to explain the occurrence of CFH-AA in aHUS with special attention to the strong association of autoimmune aHUS with homozygous deficiency of CFHR1. In the upper part of the figure phenotype of normal and CFHR1 deficient individuals are shown schematically to indicate the structural difference observed between the CFH-AA site and the corresponding site on CFHR1 (dark gray protrusion). In the novel "induced neoepitope model" binding of a ligand to domain 20 of CFH, such as a microbial protein, induces a conformational change in the loop R1182-L1189 of the domain 20 thereby making its conformation similar to that on CFHR1 domain 5.

**Figure 1**

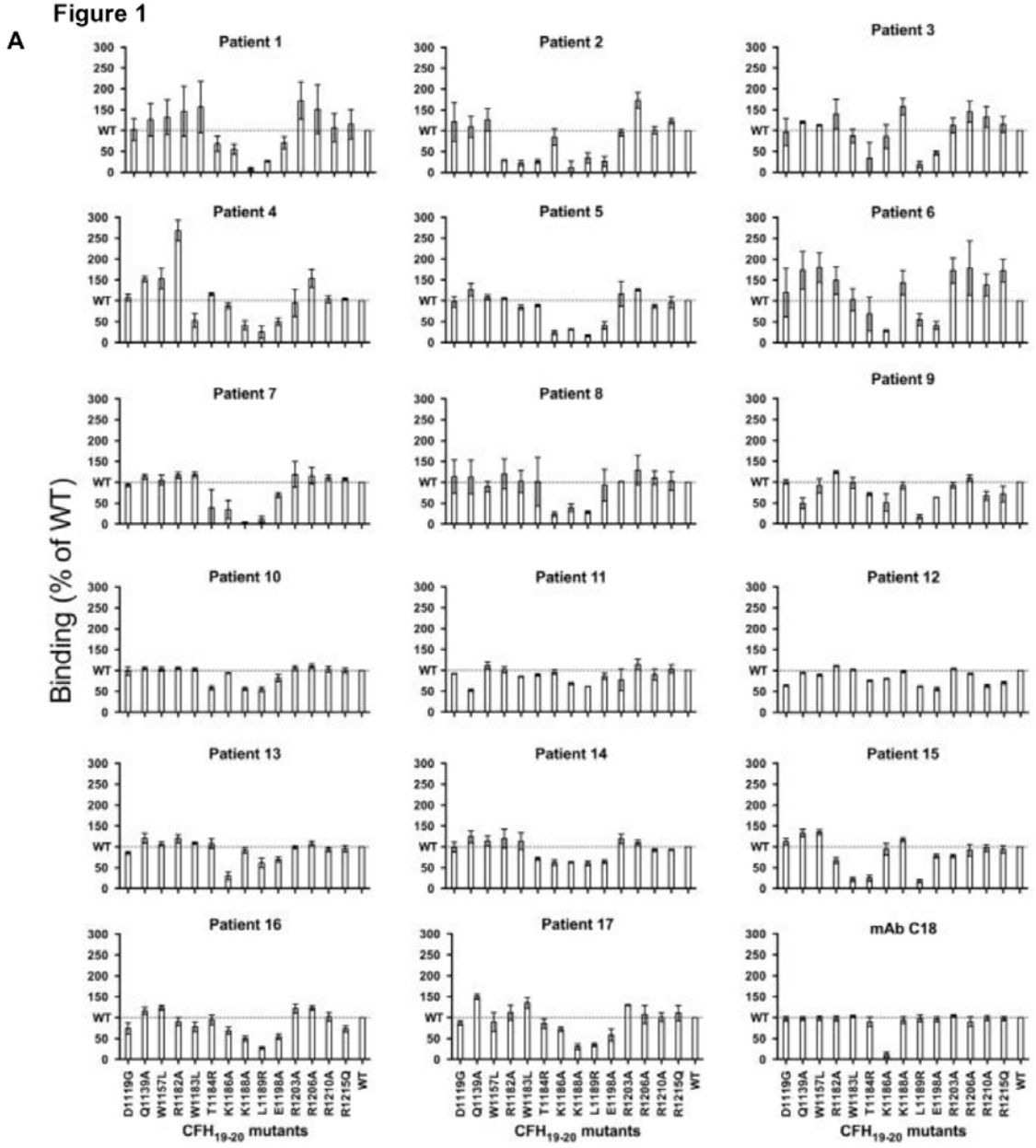
A
Patient 1
Patient 2
Patient 3
Patient 4
Patient 5
Patient 6
Patient 7
Patient 8
Patient 9
Patient 10
Patient 11
Patient 12
Patient 13
Patient 14
Patient 15
Patient 16
Patient 17
mAb C18
Binding (% of WT)
WT
D1119G
Q1139A
W1157L
R1182A
W1183L
T1184R
K1186A
K1188A
L1189R
E1198A
R1203A
R1206A
R1210A
R1215Q
CFH19-20 mutants

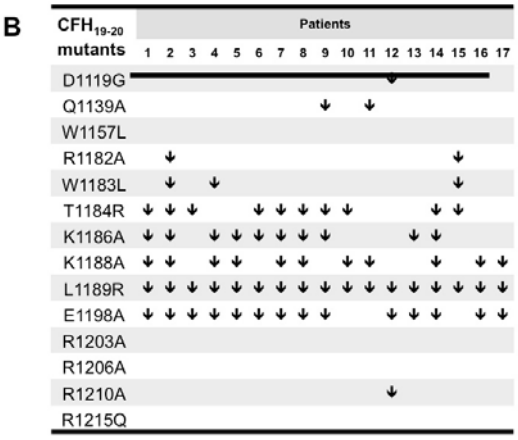
B
CFH19-20 mutants
Patients
1 2 3 4 5 6 7 8 9 10 11 12 13 14 15 16 17
D1119G
Q1139A
W1157L
R1182A
W1183L
T1184R
K1186A
K1188A
L1189R
E1198A
R1203A
R1206A
R1210A
R1215Q

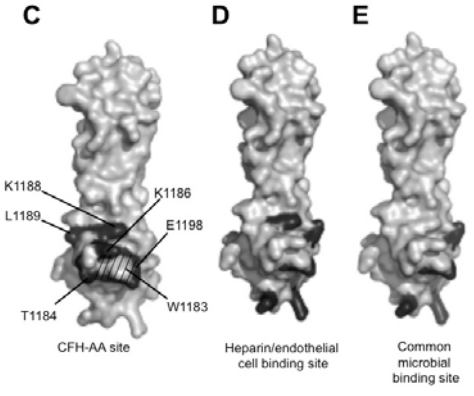
C
D
E
K1188
K1186
L1189
E1198
T1184
W1183
CFH-AA site
Heparin/endothelial cell binding site
Common microbial binding site

**Figure 2**

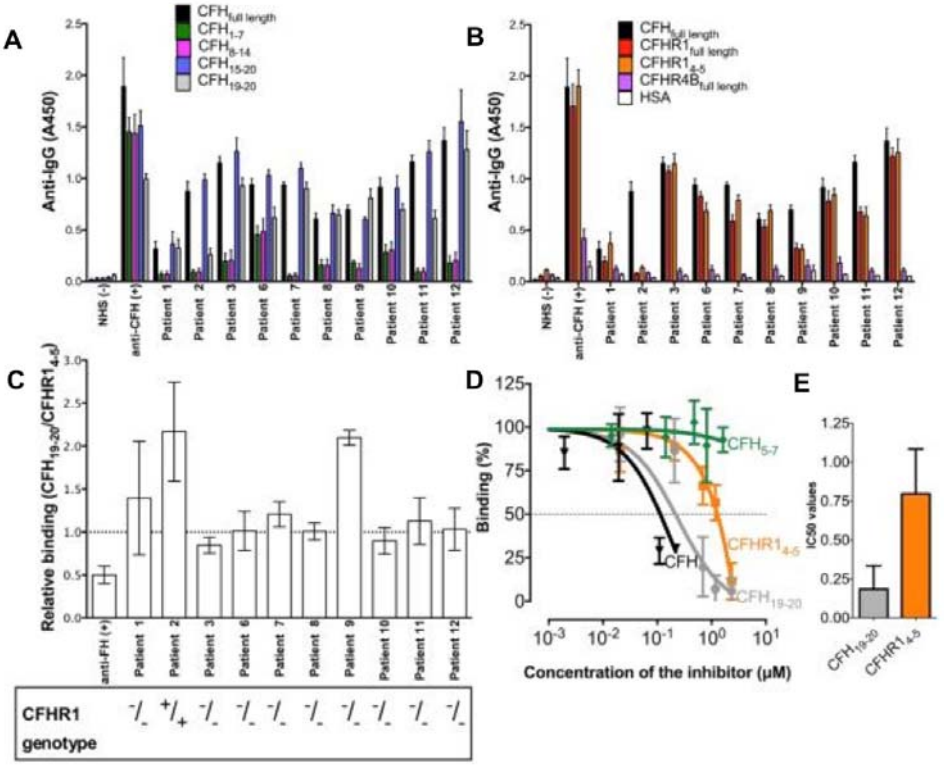
A
B
C
D
E
Anti-IgG (A450)
Relative binding (CFH19-20/CFHR14-5)
Binding (%)
Concentration of the inhibitor (µM)
IC50 values
CFHR1 genotype
NHS (-)
anti-CFH (+)
anti-FH (+)
Patient 1
Patient 2
Patient 3
Patient 6
Patient 7
Patient 8
Patient 9
Patient 10
Patient 11
Patient 12
HSA

**Figure 3**

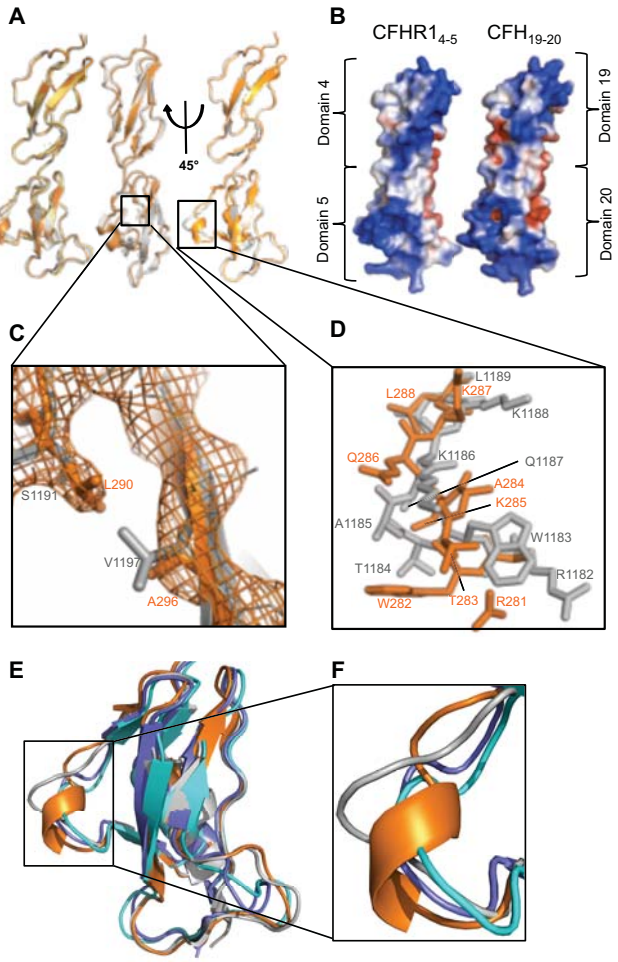
A
45°
B
CFHR1$_{4-5}$
CFH$_{19-20}$
Domain 4
Domain 5
Domain 19
Domain 20
C
S1191
L290
V1197
A296
D
L1189
L288
K287
K1188
Q286
K1186
Q1187
A284
K285
A1185
W1183
T1184
R1182
W282
T283
R281
E
F

**Figure 4**

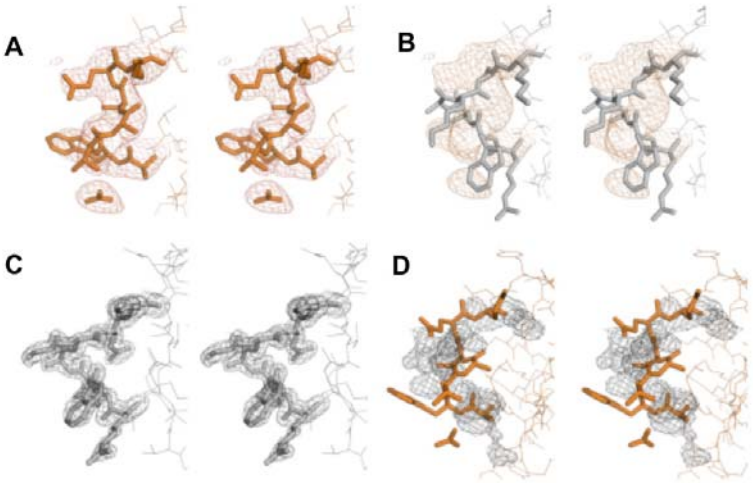

**Figure 5**

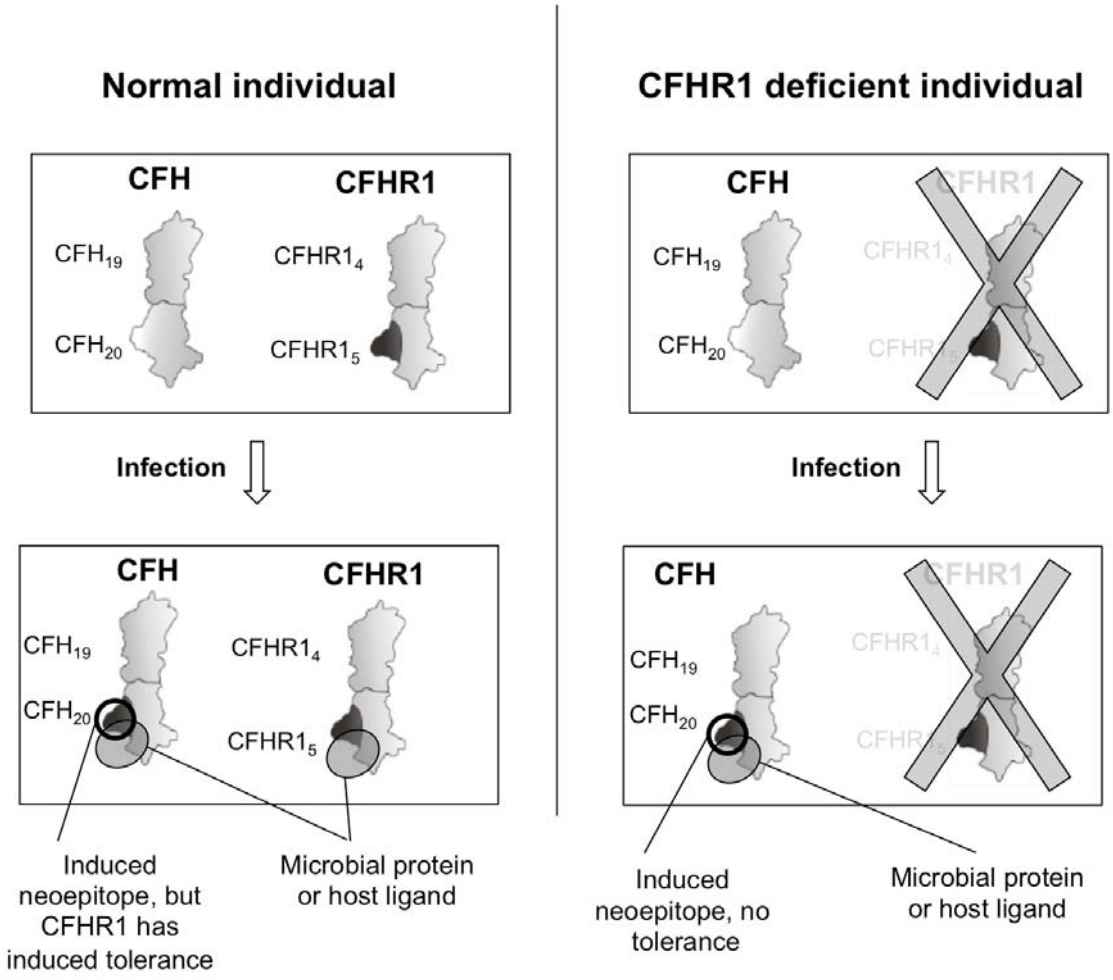
Normal individual
CFH
CFHR1
CFH19
CFH20
CFHR14
CFHR15
Infection
CFH
CFHR1
CFH19
CFH20
CFHR14
CFHR15
Induced neoepitope, but CFHR1 has induced tolerance
Microbial protein or host ligand
CFHR1 deficient individual
CFH
CFHR1
CFH19
CFH20
CFHR14
CFHR15
Infection
CFH
CFHR1
CFH19
CFH20
CFHR14
CFHR15
Induced neoepitope, no tolerance
Microbial protein or host ligand